Momilactone B induces apoptosis and G1 arrest of the cell cycle in human monocytic leukemia U937 cells through downregulation of pRB phosphorylation and induction of the cyclin-dependent kinase inhibitor p21$^{Waf1/Cip1}$

CHEOL PARK[1], NA YOUNG JEONG[2], GI-YOUNG KIM[3], MIN HO HAN[4,5], ILL-MIN CHUNG[6], WUN-JAE KIM[7], YOUNG HYUN YOO[2] and YUNG HYUN CHOI[4,5]

[1]Department of Molecular Biology, College of Natural Sciences, Dongeui University, Busan 614-714; [2]Department of Anatomy and Cell Biology, Dong-A University College of Medicine and Mitochondria Hub Regulation Center, Busan 602-714; [3]Laboratory of Immunobiology, Department of Marine Life Sciences, Jeju National University, Jeju 690-756; [4]Department of Biochemistry, Dongeui University College of Oriental Medicine, Busan 614-052; [5]Anti-Aging Research Center and Blue-Bio Industry Regional Innovation Center, Dongeui University, Busan 614-714; [6]Department of Applied Life Science, College of Life and Environmental Science, Konkuk University, Seoul 143-701; [7]Department of Urology, Chungbuk National University College of Medicine, Cheongju 361-763, Republic of Korea

Received November 30, 2013; Accepted January 14, 2014

DOI: 10.3892/or.2014.3008

Abstract. Momilactone B, a terpenoid phytoalexin present in rice bran, has been shown to exhibit several biological activities. The present study was conducted using cultured human leukemia U937 cells to elucidate the possible mechanisms by which momilactone B exerts its anticancer activity, which to date has remained poorly understood. Momilactone B treatment of U937 cells resulted in a dose-dependent inhibition of cell growth and induced apoptotic cell death as detected by chromatin condensation, DNA fragmentation, the cleavage of poly(ADP-ribose) polymerase and Annexin V-FITC staining. Flow cytometric analysis revealed that momilactone B resulted in G1 arrest in cell cycle progression, which was associated with the dephosphorylation of retinoblastoma protein (pRB) and enhanced binding of pRB with the E2F transcription factor family proteins. Treatment with momilactone B also increased the expression of cyclin-dependent kinase (Cdk) inhibitor p21$^{Waf1/Cip1}$ in a p53-independent manner, without any noticeable changes in G1 cyclins and cyclin-dependent kinases (Cdks), except a slight decrease in cyclin E. Moreover, *in vitro* kinase assay indicated that momilactone B significantly decreased Cdk4- and Cdk6-associated kinase activities through a notably increased binding of p21 to Cdk4 and Cdk6. Our results demonstrated that momilactone B caused G1 cell cycle arrest and apoptosis in U937 cells through the induction of p21 expression, inhibition of Cdk/cyclin-associated kinase activities, and reduced phosphorylation of pRB, which may be related to anticancer activity.

Correspondence to: Dr Young Hyun Yoo, Department of Anatomy and Cell Biology, Dong-A University College of Medicine and Mitochondria Hub Regulation Center, Busan 602-714, Republic of Korea
E-mail: yhyoo@dau.ac.kr

Dr Yung Hyun Choi, Department of Biochemistry, Dongeui University College of Oriental Medicine, Busan 614-052, Republic of Korea
E-mail: choiyh@deu.ac.kr

Key words: momilactone B, U937 cells, G1 arrest, apoptosis, pRB, p21

Introduction

Impaired deregulated cell cycle progression and induction of apoptosis are the primary characteristics of cancer cells due to an imbalance between proliferation and cell death. In terms of cell cycle regulation, the cyclin-dependent kinases (Cdks) are the key regulators of eukaryotic cell cycle progression in cooperation with various endogenous cyclins and Cdks (1,2). An alteration in the cooperation may lead to increased or decreased cell growth and proliferation followed by differentiation and/or cell death by apoptosis (3,4). Therefore, the key regulators of cell cycle progression and apoptotic induction may be important molecular targets for therapeutic intervention, and inhibition of cell cycle regulation may be particularly useful in the treatment of diseases caused by uncontrolled cell proliferation, such as cancer.

In general, passage through G1 into the S phase is regulated by the activities of D-type cyclin- and cyclin E-associated Cdks. D-type cyclins bind to existing Cdk4 and Cdk6, forming active complexes. The complexes in turn phosphorylate the retinoblastoma susceptibility protein (pRB). The hyperphosphorylated pRB dissociates from the E2F/DP1/pRB

complex, which was bound to the E2F responsive genes, effectively 'blocking' them from transcription and activating E2F. The activation of E2F results in the transcription of various genes, such as cyclin E, cyclin A and DNA polymerase (5,6). The accumulation of cyclin E is highly periodic, peaking during the late G1 and declining in the S phase, forming the cyclin E/Cdk2 complex, which pushes the cell from the G1 to the S phase and initiates G2/M transition (7,8). The activation of cyclin A/Cdk2 following that of cyclin E/Cdk2 is also essential for S phase progression. In addition, cyclin B/Cdc2 complex activation causes the breakdown of the nuclear envelope and the initiation of prophase and, subsequently, its deactivation causes the cell to exit mitosis (8,9).

Phytoalexins are low-molecular-weight compounds that are synthesized by, and accumulated in plants after their exposure to microorganisms (10,11). Among them, momilactone B, a terpenoid phytoalexin commonly biosynthesized from geranylgeranyl diphosphate, was originally isolated from rice (*Oryza sativa* L.) hulls as a growth inhibitor involved in seed dormancy (12,13). Although this compound has been studied as an allelochemical of rice (14,15), several reports have revealed that momilactone B exhibits several biological activities as a potential herbicidal agent (16,17). More recently, momilactone B has been shown to be a novel potential chemotherapeutic agent to induce apoptosis in solid human tumors and blood cancer cells (18,19). However, the anticancer effects of momilactone B have not been well investigated.

In the course of our screening for novel modulators of cell cycle progression and apoptotic induction as anticancer drug candidates, the present study was designed to investigate the cellular mechanisms of momilactone B-mediated antiproliferative activity in human monocytic leukemia U937 cells. Accordingly, in the present study, we found that momilactone B induced cell cycle arrest at the G1 phase and apoptotic cell death in U937 cells.

Materials and methods

Cell culture, momilactone B treatment and 3-(4,5-dimethylthiazol-2-yl)-2,5-diphenyltetrazolium bromide (MTT) assay. Human leukemia U937 cells were purchased from the American Type Culture Collection (Rockville, MD, USA) and cultured in RPMI-1640 medium (Invitrogen Corp., Carlsbad, CA, USA) and supplemented with 10% (v/v) fetal bovine serum (FBS; Gibco-BRL, Grand Island, NY, USA), 1 mM L-glutamine, 100 U/ml penicillin and 100 mg/ml streptomycin at 37˚C in a humidified atmosphere of 95% air and 5% CO_2. Momilactone B (Fig. 1) was kindly provided by Professor Chung of the Department of Applied Life Science, Konkuk University College of Life and Environmental Science (Seoul, Korea) and dissolved in dimethyl sulfoxide (DMSO; Sigma-Aldrich Chemical Co., St. Louis, MO, USA) to a stock concentration (10 mg/ml), and stored at -80˚C until use. The DMSO concentration did not exceed 0.05%. An MTT (Sigma-Aldrich) assay was performed to determine cell viability. Briefly, cells were seeded in 6-well culture plates at a density of $1x10^5$ cells/well and incubated for 24 h. Thereafter, momilactone B at various concentrations up to 2 μg/ml, as indicated, was added to the medium for 48 h to evaluate the dose-dependent effect of momilactone B on cell viability. After incubation, 400 μg/ml of MTT solution was added and incubation was carried out for 1 h. The medium was then aspirated, and the dark blue crystal product was extracted with DMSO. Colorimetric change was read on a microtiter plate reader with a 570-nm filter and a reference wavelength of 430 nm.

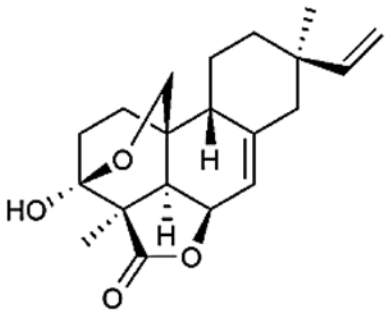

Figure 1. Chemical structure of momilactone B.

Cell cycle analysis. The cell cycle distribution at each phase of the cell cycle was assessed according to the percentage of cells with DNA content using the propidium iodide (PI; Sigma-Aldrich) staining technique. Briefly, cells were washed twice with ice-cold phosphate-buffered saline (PBS), harvested, fixed with ice-cold PBS in 70% ethanol, and then stored at 4˚C for 24 h. For flow cytometric analysis, the cells were incubated with 0.1 mg/ml RNase A (Sigma-Aldrich) for 30 min at 37˚C, stained with 50 μg/ml PI for 30 min on ice, and then measured using a FACSCalibur flow cytometer (Becton-Dickinson, San Diego, CA, USA) with CellQuest software (20).

DNA fragmentation assay. For the detection of DNA fragmentation, cells were lysed in a solution [10 mM Tris-HCl pH 7.4, 150 mM NaCl, 5 mM ethylenediaminetetraacetic acid (EDTA) and 0.5% Triton X-100] at room temperature for 20 min. The lysates were vortexed and cleared by centrifugation at 14,000 rpm for 20 min. The DNA in the supernatant was extracted using a 25:24:1 (v/v/v) equal volume of neutral phenol:chloroform:isoamyl alcohol and analyzed electrophoretically on 1.0% agarose gels containing 0.1 μg/ml ethidium bromide (EtBr) (both from Sigma-Aldrich).

Morphological observation of nuclear change. After being cultured with various concentrations of momilactone B for 48 h, cells were washed with PBS and fixed with 3.7% paraformaldehyde in PBS for 10 min at room temperature. Fixed cells were washed with PBS, and stained with 4,6-diamidino-2-phenylindole (DAPI; Sigma-Aldrich) solution for 10 min at room temperature. The cells were analyzed using a fluorescence microscope (Carl Zeiss, Germany).

Assessment of apoptosis by flow cytometry. To assess the induced cell apoptosis rate quantitatively, fluorescein-conjugated Annexin V (Annexin V-FITC) staining assay was performed according to the manufacturer's protocol (BD Biosciences Pharmingen, San Jose, CA, USA). Briefly, cells were stained with 5 μl Annexin V-FITC and 5 μl PI in each sample. After incubation for 15 min at room temperature in the

Table I. Gene-specific primers for RT-PCR.

Name		Primer sequences
Cyclin D1	Sense	5'-TGG ATG CTG GAG GTC TGC GAG GAA-3'
	Antisense	5'-GGC TTC GAT CTG CTC CTG GCA GGC-3'
Cyclin E	Sense	5'-AGT TCT CGG CTC GCT CCA GGA AGA-3'
	Antisense	5'-TCT TGT GTC GCC ATA TAC CGG TCA-3'
Cdk2	Sense	5'-GCT TTC TGC CAT TCT CAT CG-3'
	Antisense	5'-GTC CCC AGA GTC CGA AAG AT-3'
Cdk4	Sense	5'-ACG GGT GTA AGT GCC ATC TG-3'
	Antisense	5'-TGG TGT CGG TGC CTA TGG GA-3'
Cdk6	Sense	5'-CGA ATG CGT GGC GGA GAT C-3'
	Antisense	5'-CCA CTG AGG TTA GAG CCA TC-3'
p16	Sense	5'-CGG AAG GTC CCT CAG ACA TC-3'
	Antisense	5'-TCA TGA AGT CGA CAG CTT CCG-3'
p21	Sense	5'-CTC AGA GGA GGC GCC ATG-3'
	Antisense	5'-GGG CGG ATT AGG GCT TCC-3'
p27	Sense	5'-AAG CAC TGC CGG GAT ATG GA-3'
	Antisense	5'-AAC CCA GCC TGA TTG TCT GAC-3'
GAPDH	Sense	5'-CGG AGT CAA CGG ATT TGG TCG TAT-3'
	Antisense	5'-AGC CTT CTC CAT GGT GGT GAA GAC-3'

dark, the degree of apoptosis was quantified as a percentage of the Annexin V-positive and PI-negative cells by flow cytometry (21).

Reverse transcription-polymerase chain reaction (RT-PCR) analysis. The mRNA expression of cell cycle-regulated genes was examined using RT-PCR. Total RNA was extracted from the cells using TRIzol reagent (Invitrogen). Single-stranded cDNAs were synthesized with oligo(dT) primers in a reaction, starting with 2 μg of total RNA using M-MLV reverse transcriptase (Promega, Madison, WI, USA) according to the manufacturer's protocol. PCR amplification was carried out in a 25 μl total volume containing 2 μl cDNA, 200 μM each dNTP, 0.25 units *Taq* polymerase and 1 μM of each primer (Table I). Reaction conditions were optimized as follows: activation at 95˚C for 5 min, followed by 30-35 cycles at 94˚C for 45 sec, 55-64˚C for 45 sec and 72˚C for 1 min. PCR products were resolved electrophoretically on a 1.0% agarose gel and visualized by staining with EtBr.

Immunoprecipitation and western blot analysis. To prepare the whole cell extract, the cells were washed with PBS and suspended in a protein lysis buffer [25 mM Tris-Cl (pH 7.5), 250 mM NaCl, 5 mM EDTA, 1% Nonidet P-40, 0.1 mM sodium orthovanadate, 2 mg/ml leupeptin, 100 mg/ml phenylmethylsulfonyl fluoride and proteinase inhibitors]. The protein content was determined with a Bio-Rad protein assay reagent (Bio-Rad Laboratories, Hercules, CA, USA) using bovine serum albumin as the standard, following the procedure described by the manufacturer. For immunoprecipitation, 500 μg protein equivalent of the cell lysate was incubated with an indicated antibody in extraction buffer for 1 h at 4˚C. The immuno-complex was collected on protein G/A-Sepharose beads (Sigma-Aldrich). For the western blot analysis, equal amounts of cell lysate and immunoprecipitated proteins were separated by electrophoresis on sodium dodecyl sulfate (SDS)-polyacrylamide gels and transferred to nitrocellulose membranes (Schleicher & Schuell, Keene, NH, USA) by electroblotting. Each membrane was probed with the appropriate primary antibody for 1 h, incubated with the diluted enzyme-linked secondary antibody, and then visualized by enhanced chemiluminescence (ECL; Amersham Co., Arlington Heights, IL, USA) according to the recommended procedure. Antibodies against poly(ADP-ribose) polymerase (PARP), cyclin D1, cyclin E, Cdk2, Cdk4, Cdk6, pRB, E2F-1, E2F-4, p16, p21 and p27 were purchased from Santa Cruz Biotechnology, Inc. (Santa Cruz, CA, USA). Antibody against actin was obtained from Sigma-Aldrich. Peroxidase-labeled goat anti-rabbit immunoglobulin and FITC-conjugated donkey anti-rabbit IgG were purchased from Amersham Co. and Sigma-Aldrich, respectively.

Immune-complex kinase assay. Cell lysates from untreated and momilactone B-treated cells were incubated with the primary antibody for 1 h at 4˚C. Immune-complexes were collected on protein A-Sepharose beads and resuspended in kinase assay mixture containing [λ-^{32}P]ATP (ICN Biochemicals, Irvine, CA, USA) and histone H1 (Sigma-Aldrich) as substrate. After incubation at 37˚C for 30 min, the reaction was stopped by the addition of the same amount of 2X SDS sample buffer. After boiling and spinning, the samples were separated on 10% SDS-polyacrylamide gels and dried, and bands were detected by autoradiography.

Statistical analysis. The experiments were repeated three times, and the results are expressed as means ± standard deviation (SD). A one-way analysis of variance (ANOVA) followed by Dunnett's t-test was applied to assess the statistical significance of the difference among the study groups. A value of $p<0.05$ was considered to be statistically significant.

Results

Momilactone B inhibits cell viability and induces G1 phase arrest in U937 cells. To determine the inhibitory effect of momilactone B on the proliferation of U937 cells, we treated the cells with various concentrations of momilactone B for 48 h and measured cell viability using the MTT assay. As shown in Fig. 2A, momilactone B concentration-dependently led to a reduction in cell viability of U937 cells. We next investigated whether momilactone B targets cell cycle regulation in U937 cells using flow cytometric analysis. Compared with the untreated control, momilactone B-treated cells were accumulated in the G1 phase of the cell cycle in a concentration-dependent manner (Fig. 2B), which was accompanied by a decrease in the number of cells in the S and G2/M phases. Collectively, the data appear to suggest that momilactone B arrests cells in the G1 phase and thus inhibits them from entering the S and G2/M phases.

Momilactone B induces apoptosis in U937 cells. To determine whether the decrease in cell viability and G1 arrest were

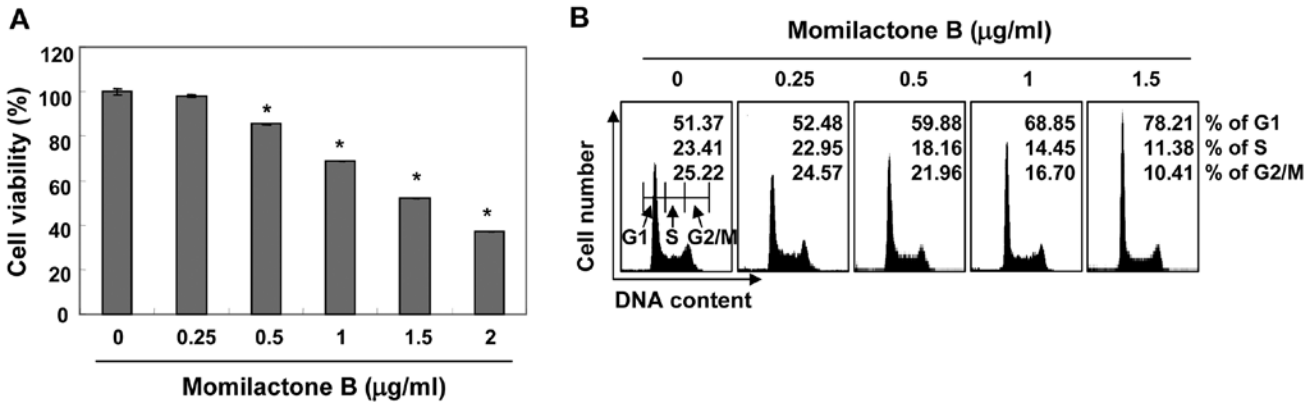

Figure 2. Momilactone B inhibits cell viability and induces G1 arrest in U937 cells. (A) Cells were treated with the indicated concentrations of momilactone B for 48 h. Cell viability was determined by MTT assay. The data are expressed as means ± SD of three independent experiments. Statistical significance was determined by the Student' t-test (*p<0.05 vs. untreated control). (B) After treatment with momilactone B for 48 h, cells were harvested and 10,000 events were analyzed for each sample. DNA content is represented on the x-axis and the number of cells counted is represented on the y-axis. Each point represents the mean of two independent experiments.

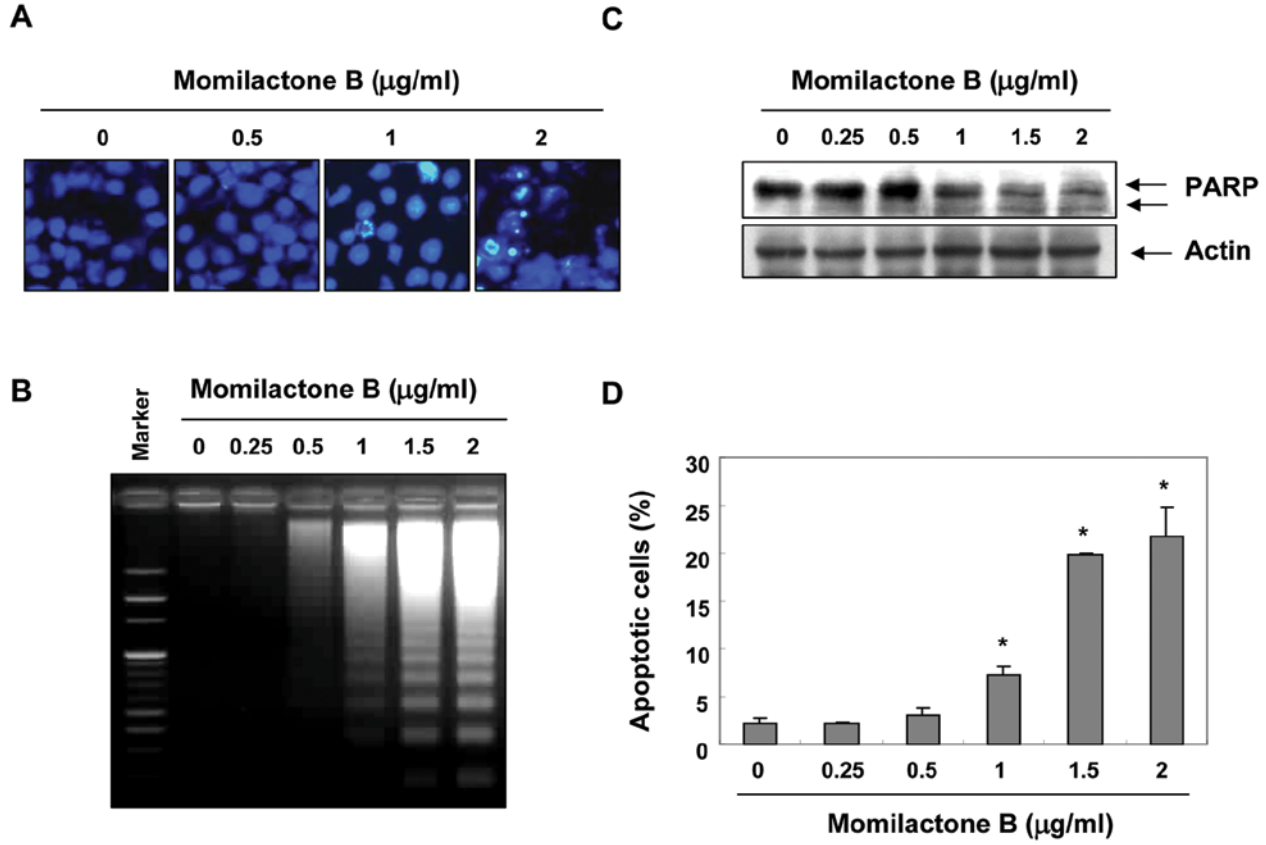

Figure 3. Induction of apoptosis by momilactone B in U937 cells. Cells were treated with the indicated concentrations of momilactone B for 48 h. (A) Cells were fixed, stained with DAPI solution, and examined by fluorescence microscopy (x400). (B) DNA fragmentation was examined by 1.0% agarose gel electrophoresis of genomic DNA, followed by EtBr staining. (C) Cell lysates were resolved on SDS-polyacrylamide gels and subjected to western blotting. The proteins were visualized using the anti-PARP antibody and an ECL detection system. Actin was used as an internal control. (D) To quantify the degree of apoptosis induced by momilactone B, the cells were stained with Annexin V, and the percentages of apoptotic cells were then analyzed using flow cytometric analysis. Each point represents the means ± SD of three independent experiments. Statistical significance was determined using the Student's t-test (*p<0.05 vs. untreated control). DAPI, 4,6-diamidino-2-phenylindole; EtBr, ethidium bromide.

associated with induction of apoptosis, we assessed the apoptosis parameters of U937 cells in response to momilactone B treatment. As shown in Fig. 3A, the nuclear structure of the control cells remained intact, whereas nuclear chromatin condensation and fragmentation, characteristics of apoptosis, were increased in a concentration-dependent manner in cells treated with momilactone B, which was associated with increased DNA fragmentation (Fig. 3B). Under the same

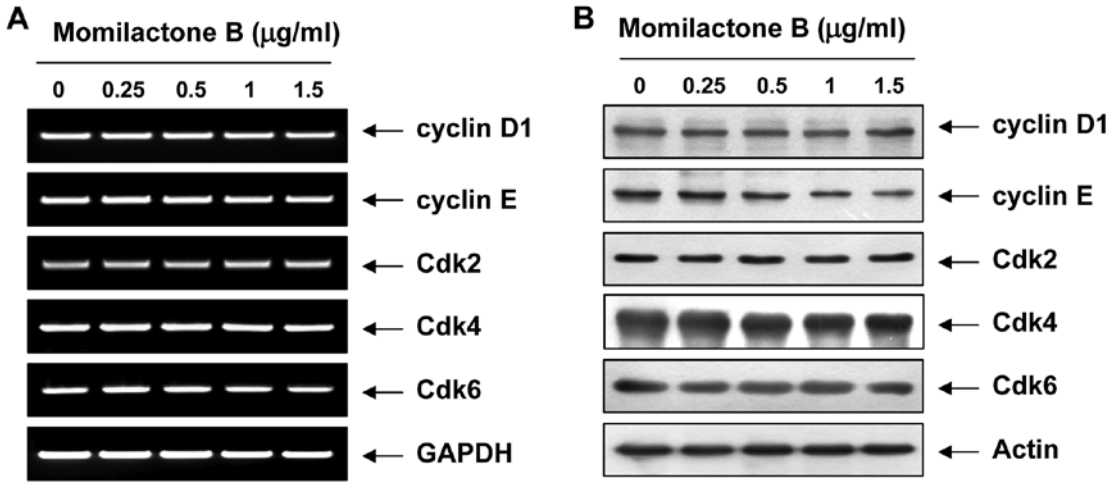

Figure 4. Effects of momilactone B on the levels of G1-associated cyclins and Cdks in U937 cells. (A) After treatment with various concentrations of momilactone B for 48 h, total RNAs were isolated and reverse-transcribed. The resulting cDNAs were then subjected to PCR with the indicated primers, and the reaction products were separated on 1.0% agarose gel and visualized by EtBr staining. (B) The cell lysates were prepared, and equal amounts of total cell lysates were subjected to SDS-polyacrylamide gel electrophoresis, transferred and probed with the indicated antibodies. Glyceraldehyde-3'-phosphate dehydrogenase (GAPDH) and actin were used as internal controls for the RT-PCR and western blot assays, respectively. Cdks, cyclin-dependent kinases; EtBr, ethidium bromide; RT-PCR, reverse transcription-polymerase chain reaction.

conditions, cleavage of the pro-form PARP protein (116 kDa) to the inactive form (85 kDa), which is an activated caspase-3 substrate, was also present (Fig. 3C). Furthermore, to measure apoptotic cell death upon momilactone B treatment, we stained cells for Annexin V and found that the percentages of apoptotic cells increased from ~2.2 to 19.8% and 21.7% after treatment with 1.5 μg/ml and 2.0 μg/ml of momilactone B, respectively, for 48 h. These results indicate that the inhibition of cell viability and G1 phase arrest of the cell cycle observed in response to momilactone B was associated with the induction of apoptosis.

Effects of momilactone B on the expression of G1 phase-associated cyclins and Cdks in U937 cells. To examine the molecular mechanisms of G1 arrest in U937 cells treated with momilactone B, we determined the expression of G1 phase regulators using RT-PCR and western blot analyses. As illustrated in Fig. 4, momilactone B partially suppressed the expression of cyclin E proteins; however, momilactone B did not significantly affect the levels of cyclin D1, Cdk2, Cdk4, and Cdk6 at both the transcriptional and translational levels.

Momilactone B downregulates pRB phosphorylation and increases the binding of pRB with E2Fs in U937 cells. Since the Rb gene product pRB is an important checkpoint protein in the G1 phase of the cell cycle, we next determined the kinetics between the phosphorylation of pRB and the transcription factors, E2Fs, in momilactone B-treated cells. As indicated in Fig. 5A, momilactone B changed the hyperphosphorylated form to a hypophosphorylated form of pRB and these changes occurred in a concentration-dependent manner, whereas the levels of E2F-1 and E2F-4 expression remained unchanged. Furthermore, co-immunoprecipitation analysis indicated that the association between pRB and E2F-1/E2F-4 was very low in the untreated control cells; however, a strong increase in the association between pRB and E2F-1 as well as E2F-4 was observed in the momilactone B-treated U937 cells (Fig. 5B).

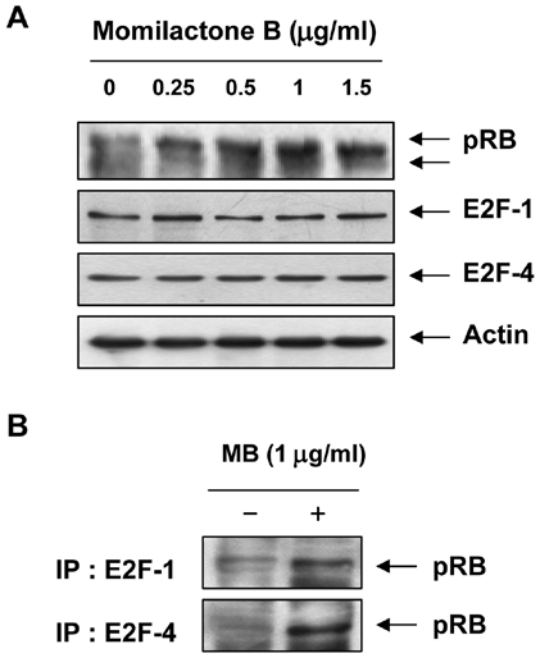

Figure 5. Induction of hypophosphorylation of pRB and enhanced association of pRB and E2Fs by momilactone B in U937 cells. (A) Following treatment with various concentrations of momilactone B for 48 h, the total cell lysates were prepared and separated by electrophoresis on an 8 or 10% SDS-polyacrylamide gel. Western blotting was then performed using anti-pRB, anti-E2F-1 and anti-E2F-4 antibodies. Actin was used as an internal control. (B) Cells were incubated without or with 1 μg/ml momilactone B (MB) for 48 h, and then equal amounts of proteins were immunoprecipitated with the anti-E2F-1 or anti-E2F-4 antibody. Immuno-complexes were separated by 8% SDS-polyacrylamide gel electrophoresis, transferred to a nitrocellulose membrane, and probed with the anti-pRB antibody. Proteins were detected by ECL detection. IP, immunoprecipitation; pRB, retinoblastoma protein; ECL, enhanced chemiluminescence.

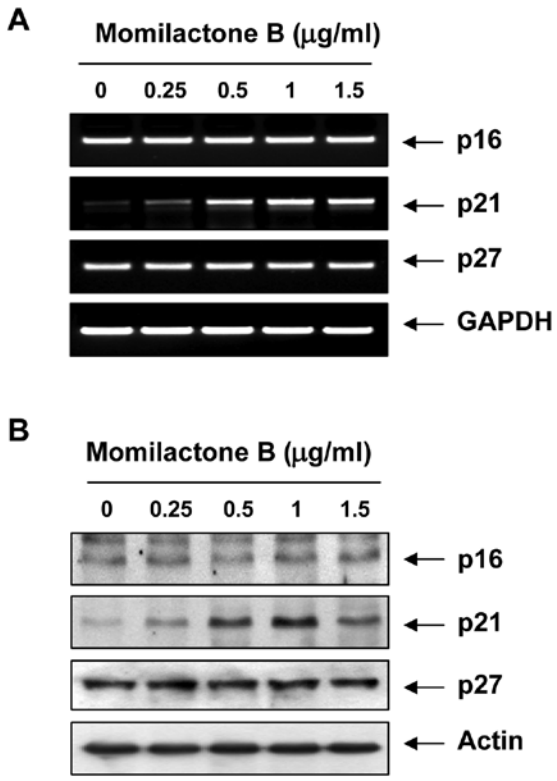

Figure 6. Effects of momilactone B on the levels of Cdk inhibitors in U937 cells. (A) Total RNAs were isolated and reverse-transcribed and resulting cDNAs were then subjected to PCR. The reaction products were subjected to electrophoresis on a 1.0% agarose gel and visualized by EtBr staining. (B) Following incubation with momilactone B under the same conditions, the cell lysates were prepared, and equal amounts of total cell lysates were subjected to SDS-polyacrylamide gel electrophoresis, transferred, and then probed with antibodies against p16, p21 and p27. GAPDH and actin were used as internal controls for the RT-PCR and western blot assays, respectively. EtBr, ethidium bromide; GAPDH, glyceraldehyde-3'-phosphate dehydrogenase.

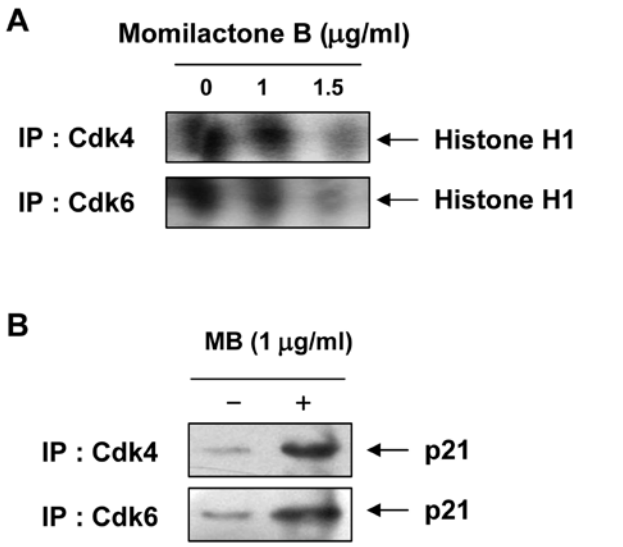

Figure 7. Inhibition of Cdk kinase activity and increased association of p21 with Cdks by momilactone B in U937 cells. (A) Following treatment with 1 μg/ml momilactone B for 48 h, total cell lysates were prepared and immunoprecipitated with the anti-Cdk4 or anti-Cdk6 antibody, and kinase activity was assayed using histone H1 as substrate. (B) The total cell lysates were prepared and immunoprecipitated with the anti-Cdk4 or anti-Cdk6 antibody, separated on 12% SDS-polyacrylamide gels, and transferred onto nitrocellulose membranes. Western blot analyses were probed with the anti-p21 antibody and an ECL detection system. Cdks, cyclin-dependent kinases; ECL, enhanced chemiluminescence; IP, immunoprecipitation.

Momilactone B induces Cdk inhibitor p21 expression in U937 cells. Since Cdk activity is highly regulated by association with Cdk inhibitors, we next examined the possible upregulation of these gene products in the U937 cells. As shown in Fig. 6, the levels of Cdk inhibitor p21 were markedly increased at the transcriptional and translational levels in a concentration-dependent manner, whereas the levels of other Cdk inhibitors, such as p16 and p27, were not altered following the same treatment. As the p53 gene is deleted in U937 cells (22), it is most likely that the induction of p21 by momilactone B was mediated in a p53-independent manner.

Momilactone B inhibits Cdks-associated kinase activity through association of p21 with Cdks in U937 cells. Since momilactone B treatment perturbed the G1 phase of the cell cycle, and the kinase activity of Cdk4 and Cdk6 plays an essential role in G1 to S phase transition, the possible effects of momilactone B on the modulation of their kinase activities were evaluated using histone H1 as the substrate. As presented in Fig. 7A, for the control cells, the high activity of the phosphorylated form of Cdk4 demonstrated the high level of histone H1 phosphorylation; however, the level of H1 phosphorylation was greatly reduced for Cdk4 in the momilactone B-treated cells. There was also a reduction in Cdk6-associated kinase activity during momilactone B treatment in a concentration-dependent manner. To further define the nature of G1 arrest following momilactone B treatment, we finally aimed to ascertain whether the p21 protein induced by momilactone B treatment was associated with Cdks. As shown in Fig. 7B, the association between p21 and Cdk4 or Cdk6 was almost undetectable in the untreated cells by co-immunoprecipitation analysis; however, treatment of cells with momilactone B resulted in a significant increase in the binding of these Cdks with p21.

Discussion

In the present study, we showed that momilactone B inhibited the proliferation of U937 cells by increasing the level of p21 expression and decreasing the phosphorylation of pRB, which in turn inhibited Cdk activity, and ultimately arrested the cell cycle at the G1 phase and induced apoptosis.

Cancer cells are characterized by the deregulation of the cell cycle and the activation of signal transduction for abnormal proliferation. In cell cycle regulation, cyclins and Cdks play important roles through the formation of the cyclin/Cdk complex and Cdk inhibitors (1,2). As cells progress through the G1 to the S phase, cyclin/Cdk complexes, such as cyclin D/Cdk4/6 and cyclin E/Cdk2 complexes, are sequentially activated along with phosphorylated pRB family proteins, such as pRB, p107 and p130, referred to as 'pocket proteins', which bind viral oncoproteins and cellular factors, such as the E2F family of transcription factors, including E2F proteins and two DP proteins (DP1 and DP2) (5,6). Among the pRB family proteins, pRB is the major negative regulator of cell division,

and pRb hyperphosphorylation is a hallmark of the G1 to S transition in the cell cycle. The hyperphosphorylated pRB releases the E2F/DP complex, which, in turn, stimulates the transcription of numerous genes whose products are required for the G1 to S transition and S phase progression (5,6). Therefore, when decreased levels of either protein or the association between respective binding partners are observed, a concomitant decrease in the degree of pRB phosphorylation would be expected. In the present study, hyperphosphorylation of the pRB family was inhibited by momilactone B (Fig. 5A), which markedly increased the binding of pRB to E2F transcription factors such as E2F-1 and E2F-4 (Fig. 5B). The data indicate that momilactone B inhibits the phosphorylation of pRB, and that this inhibition represses the transcriptional activity of E2Fs for S phase entry by promoting the binding of pRB with E2Fs.

There are two families of Cdk inhibitors, the Cip/Kip (p21, p27 and p57) and INK4 (p16, p15, p18 and p19) families, both of which bind to cyclin/Cdk complexes and inhibit their kinase activities (23,24). Therefore, we examined the effects of momilactone B on several of these cell cycle regulatory molecules with western blot analysis and *in vitro* kinase assay. The present results, which reveal that momilactone B arrests the cell cycle in the G1 phase, were correlated with the upregulation of Cdk inhibitor p21 at both the transcriptional and translational levels (Fig. 6) without significantly affecting the levels of G1-associated cyclins and Cdks. Although p16 and p27 are reported to be upregulated in response to various antiproliferative signals (25,26), they were consistently unaltered in the U937 cells. We also determined Cdk4- and Cdk6-associated kinase activities using their immunoprecipitates and histone H1 as substrates. The results from the immunocomplex kinase assays demonstrated that momilactone B downregulates both Cdk4- and Cdk6-associated activities, rather than altering the protein levels (Fig. 7A). In addition, co-immunoprecipitation analysis indicated that treatment of cells with momilactone B resulted in a significant increase in the binding of Cdk4 and Cdk6 with p21, indicating that the inhibition of Cdk kinase activity may involve the binding of the Cdk inhibitor protein p21 to the cyclin/Cdk complexes. Taken together, these results indicate that momilactone B treatment inhibited cyclin D/Cdk4/6 kinase activities, which led to a reduction in the level of pRB phosphorylation and thereby, G1 cell cycle arrest in U937 cells. In addition, the momilactone B-induced reduction in the cyclin/Cdk kinase activities may be due to the upregulation of Cdk inhibitor p21. Although the ability of p21 is known to be induced through tumor suppressor gene p53-dependent and -independent pathways (27,28), the momilactone B-induced upregulation of p21 in U937 cells appears to be independent of p53 since the U937 cell line is a p53-null leukemia cell line (22).

In conclusion, the present study demonstrated that momilactone B induces G1 phase arrest and apoptosis in U937 cells. The G1 cell cycle arrest was mediated by inhibiting pRB phosphorylation and enhanced complex formation between pRB and the transcription factor E2Fs. Treatment with momilactone B resulted in the inhibition of Cdk4/6 kinase activity as well as enhanced binding with p21 and Cdk4/6 accompanied by p53-independent induction of the Cdk inhibitor, p21. These novel phenomena have not been previously described and suggest that momilactone B may have significant potential for development as a cancer treatment.

Acknowledgements

This study was supported by the National Research Foundation of Korea (NRF) grant funded by the Korean government (MSIP) (nos. 2008-0062611 and 2013-041811).

References

1. Lim S and Kaldis P: Cdks, cyclins and CKIs: roles beyond cell cycle regulation. Development 140: 3079-3093, 2013.
2. Sánchez I and Dynlacht BD: New insights into cyclins, CDKs, and cell cycle control. Semin Cell Dev Biol 16: 311-321, 2005.
3. Sperka T, Wang J and Rudolph KL: DNA damage checkpoints in stem cells, ageing and cancer. Nat Rev Mol Cell Biol 13: 579-590, 2012.
4. Canavese M, Santo L and Raje N: Cyclin dependent kinases in cancer: potential for therapeutic intervention. Cancer Biol Ther 13: 451-457, 2012.
5. van den Heuvel S and Dyson NJ: Conserved functions of the pRB and E2F families. Nat Rev Mol Cell Biol 9: 713-724, 2008.
6. Sun A, Bagella L, Tutton S, Romano G and Giordano A: From G0 to S phase: a view of the roles played by the retinoblastoma (Rb) family members in the Rb-E2F pathway. J Cell Biochem 102: 1400-1404, 2007.
7. Lindqvist A, Rodríguez-Bravo V and Medema RH: The decision to enter mitosis: feedback and redundancy in the mitotic entry network. J Cell Biol 185: 193-202, 2009.
8. Porter LA and Donoghue DJ: Cyclin B1 and CDK1: nuclear localization and upstream regulators. Prog Cell Cycle Res 5: 335-347, 2003.
9. Jeong AL and Yang Y: PP2A function toward mitotic kinases and substrates during the cell cycle. BMB Rep 46: 289-294, 2013.
10. Ahuja I, Kissen R and Bones AM: Phytoalexins in defense against pathogens. Trends Plant Sci 17: 73-90, 2012.
11. Pedras MS and Ahiahonu PW: Metabolism and detoxification of phytoalexins and analogs by phytopathogenic fungi. Phytochemistry 66: 391-411, 2005.
12. Toyomasu T, Kagahara T, Okada K, Koga J, Hasegawa M, Mitsuhashi W, Sassa T and Yamane H: Diterpene phytoalexins are biosynthesized in and exuded from the roots of rice seedlings. Biosci Biotechnol Biochem 72: 562-567, 2008.
13. Wickham KA and West CA: Biosynthesis of rice phytoalexins: identification of putative diterpene hydrocarbon precursors. Arch Biochem Biophys 293: 320-332, 1992.
14. Chung IM, Kim JT and Kim SH: Evaluation of allelopathic potential and quantification of momilactone A,B from rice hull extracts and assessment of inhibitory bioactivity on paddy field weeds. J Agric Food Chem 54: 2527-2536, 2006.
15. Kato-Noguchi H and Ino T: Rice seedling release momilactone B into the environment. Phytochemistry 63: 551-554, 2003.
16. Chung IM, Hahn SJ and Ahmad A: Confirmation of potential herbicidal agents in hulls of rice, *Oryza sativa*. J Chem Ecol 31: 1339-1352, 2005.
17. Chung IM, Ali M, Ahmad A, Chun SC, Kim JT, Sultana S, Kim JS, Min SK and Seo BR: Steroidal constituents of rice (*Rryza sativa*) hulls with algicidal and herbicidal activity against blue-green algae and duckweed. Phytochem Anal 18: 133-145, 2007.
18. Lee SC, Chung IM, Jin YJ, Song YS, Seo SY, Park BS, Cho KH, Yoo KS, Kim TH, Yee SB, Bae YS and Yoo YH: Momilactone B, an allelochemical of rice hulls, induces apoptosis on human lymphoma cells (Jurkat) in a micromolar concentration. Nutr Cancer 60: 542-551, 2008.
19. Kim SJ, Park HR, Park EJ and Lee SC: Cytotoxic and antitumor activity of momilactone B from rice hulls. J Agric Food Chem 55: 1702-1706, 2007.
20. Di X, Andrews DM, Tucker CJ, Yu L, Moore AB, Zheng X, Castro L, Hermon T, Xiao H and Dixon D: A high concentration of genistein down-regulates activin A, Smad3 and other TGF-β pathway genes in human uterine leiomyoma cells. Exp Mol Med 44: 281-292, 2012.

21. Li Z and Gao Q: Induction of apoptosis in HT-29 cells by quercetin through mitochondria-mediated apoptotic pathway. Anim Cells Syst 17: 147-153, 2013.
22. Danova M, Giordano M, Mazzini G and Riccardi A: Expression of p53 protein during the cell cycle measured by flow cytometry in human leukemia. Leuk Res 14: 417-422, 1990.
23. Pavletich NP: Mechanisms of cyclin-dependent kinase regulation: structures of Cdks, their cyclin activators, and Cip and INK4 inhibitors. J Mol Biol 287: 821-828, 1999.
24. Galons H, Oumata N and Meijer L: Cyclin-dependent kinase inhibitors: a survey of recent patent literature. Expert Opin Ther Pat 20: 377-404, 2010.
25. Matsuda Y and Ichida T: p16 and p27 are functionally correlated during the progress of hepatocarcinogenesis. Med Mol Morphol 39: 169-175, 2006.
26. Lee MH and Yang HY: Negative regulators of cyclin-dependent kinases and their roles in cancers. Cell Mol Life Sci 58: 1907-1922, 2001.
27. Abbas T and Dutta A: p21 in cancer: intricate networks and multiple activities. Nat Rev Cancer 9: 400-414, 2009.
28. Gartel AL and Tyner AL: The role of the cyclin-dependent kinase inhibitor p21 in apoptosis. Mol Cancer Ther 1: 639-649, 2002.